Indian Journal of Science and Technology, *Vol 10(28), DOI: 10.17485/ijst/2017/v10i28/115333, July 2017*
ISSN (Print) : 0974-6846
ISSN (Online) : 0974-5645

Studies on the Effect of Superstrate Loading on Artificial Magnetic Conductor Characteristics

Libi Mol Vadakkekalathil Abdul Hakim* and Chandroth Karuvandi Aanandan

Microwave Propagation Research Laboratory (MPRL), Department of Electronics, Cochin University of Science and Technology, Kochi – 682022, Kerala, India; libimol_va@cusat.ac.in, anand@cusat.ac.in

Abstract

Objectives: To study the effect of superstrate loading on the performance of artificial magnetic conductor. **Methods/ Statistical Analysis**: The simulation studies on the effect of superstrate loading are carried out by using CST MW Studio-2016. For performance evaluation, the structure is fabricated by photolithography and the measurements are carried out in an anechoic environment using vector network analyzer R&S VNA ZVB 20. **Findings:** The characteristics of an AMC structure fabricated on a substrate can be altered by loading an appropriate superstrate. The thickness of the superstrate is an important factor which influences the AMC resonance frequency as well as its bandwidth. The structure presented here is polarization independent with good angular stability up to $\pm 30^0$. **Application/Improvements:** By imparting losses into the superstrate, the performance of AMC can be changed to an absorber or perfect conductor depending upon the loss.

Keywords: AMC Absorber, Artificial Magnetic Conductor, Bandwidth, Polarization Independence, Superstrate Loading

1. Introduction

Artificial magnetic conductors are metamaterial showing the reflection phase performance of Perfect Magnetic Conductors (PMC) for a particular frequency band[1]. It comprises of a periodic array of Frequency Selective Surfaces (FSS) over a metal backed dielectric layer. Due to the in-phase reflection property, AMC find applications in areas such as low profile antennas, electromagnetic absorbers[2], Fabry-Perot or leaky wave antennas[3].

Based on the equivalent circuit modeling of AMC, the resonance frequency is inversely proportional to square root of Capacitance (C) of the structure. Therefore the resonance frequency can be tuned by varying C. A method of tuning the capacitance of AMC by periodically loading the FSS elements with varactor diodes has been reported[4]. The varactor diodes can also be connected in between the FSS element and ground plane to simplify the biasing network[5]. The number of varactor diodes can be reduced by connecting the FSS elements to the feeding network placed behind the ground plane through the metalized vias[6]. The capacitance of the AMC and therefore its resonance frequency can be tuned by varying the dielectric constant of the substrate material[7]. The tunability of grapheme conductivity can also be exploited to design reconfigurable high impedance surface consisting of graphene and metal patches[8]. The dielectric is used as the superstrate in AMC structure to reduce the sensitivity of the AMC resonant frequency in the presence of rainwater[9].

In this paper, a simple method for the modification of AMC operation of a fabricated structure by superstrate loading to adapt it for specific application requirement is reported. Since the capacitance of the AMC also depends on the dielectric superstrate, resonance frequency can be altered by the changing its properties even after the AMC structure is fabricated. The different frequencies thus obtained also retain the property of polarization independent nature and angular stability. Larger thickness of superstrate gives lower resonance frequencies with better bandwidth. The effect of different properties of the superstrate is also analyzed and included in the paper. Studies on the effect of losses in the superstrate shows that the AMC on a lossless substrate can be changed to

**Author for correspondence*

an absorber using a lossy superstrate. Usually coplanar resistors or resistive films are used in AMC structures to design thin absorbers[2]. Even though this proposed lossy superstrate loaded absorber configuration has the demerit of added height and a dramatic increase in mass of AMC structure as compared to ref [2], this is the best suitable method to design an absorber from an already fabricated AMC structure.

2. Geometry and Equivalent Circuit of the Structure

The proposed structure consists of an array of square patch FSS on a grounded dielectric. The FSS unit cell with dimension 8 mm ∗ 8 mm is considered over a commercially available FR4 substrate with thickness 0.8 mm and dielectric constant 4.4–0.11j. The dimensions of the square patch is optimized as l = 5 mm to obtain the AMC characteristic at 12.39 GHz using CST MW Studio[10]. FR4 as well as other substrates with different values of thickness and permittivity are considered as superstrate.

The square patch FSS can be represented by a series inductor (L) and capacitor (C) and grounded dielectric by an inductor (L'). The superstrate loaded on the structure can be represented by a capacitor (C'). The value of C' depends on the permittivity of the material and its thickness. As the thickness of dielectric increases, the effective capacitance of the whole structure increases and results in reduction in resonance frequency. The front view of the unit cell, side view of the structure and equivalent circuit are shown in Figures 1 (a), (b) and (c) respectively.

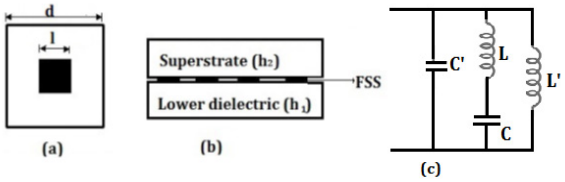

Figure 1. (a) Unit cell geometry, (b) Side view of the structure and (c) Equivalent circuit.

3. Simulation Results and Discussion

The simulation result showing the performance of AMC for FR-4 superstrate with different thickness is given in Figure 2. The simulations are carried out using the frequency domain solver in CST MW studio. The variation in resonance frequency and bandwidth with superstrate thickness are given in Table 1. These results indicate that both reduction in resonance frequency and increase in bandwidth can be obtained by increasing the superstrate thickness. To validate this property, dielectric having permittivity 2.6 and 6.6 are also considered as superstrate and the results were tabulated in Table 1. The simulated % bandwidth is shown in Table 1 and it indicates that the structure with superstrate loading is showing enhancement in bandwidth.

The effects of angle of incidence, polarization of incident wave, permittivity of superstrate, loss in the superstrate are also studied and presented in the following sections.

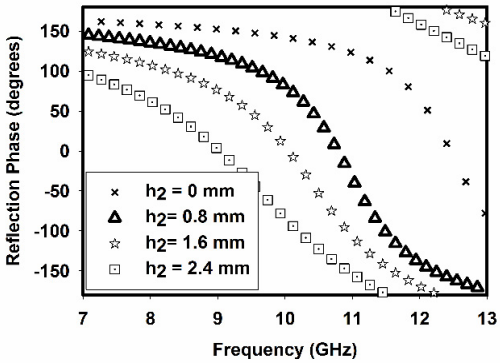

Figure 2. Effect of superstrate thickness (h_2) on AMC performance (d = 8 mm, l = 5 mm, h_1 = 0.8 mm, ε_r (super) = 4.4-j*0.11, ε_r (sub) = 4.4-j*0.11).

Table 1. The variation of resonance frequency and bandwidth with superstrate thickness (h_2)

ε_{real}	h_2 (mm)	Resonance frequency (GHz)	Bandwidth (GHz)	% Bandwidth
8	0	12.39	1.38 (11.7-13.08)	11.13
2.6	0.8	11.6	1.62 (10.59-12.21)	14.2
6	1.6	11.02	2.78(8.81-11.59)	27.25
	2.4	10.39	3.06(8.25-11.31)	31.2
4.4	0.8	10.77	1.54 (9.84-11.38)	14.51
9.	1.6	10.03	2.21 (8.62-10.83)	22.72
	2.4	9.02	2.87 (7.24-10.07)	33.16
6.6	0.8	10.11	1.51(9.21-10.72)	15.1
10	1.6	8.98	2(7.75-9.75)	22.8
	2.4	7.85	2.48(6.41-8.89)	32.41

3.1 Permittivity of the Superstrate

The effect of permittivity of the superstrate on the performance of structure is also simulated and is shown in Figure 3. The parameter h_2 is taken as 1.6 mm. It is noted that as the permittivity increases from 2.6 to 6.6, the resonant frequency decreases from 11.02 GHz to 8.98 GHz. It is due to the fact that the resonant frequency is inversely proportional to the capacitance, which is directly proportional to the permittivity.

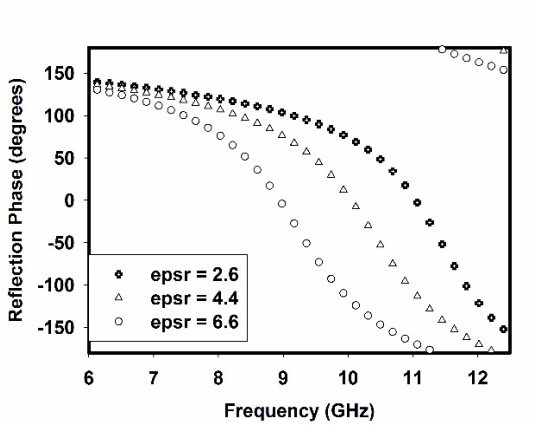

Figure 3. Effect of superstrate permittivity (ε_r) on AMC performance (d = 8 mm, l = 5 mm, h_1 = 0.8 mm, h_2 = 1.6 mm, ε_r (sub) = 4.4-j*0.11).

3.2 Loss in the Superstrate

The loss tangent (tan δ) of the superstrate is considered as 0.025 ($\varepsilon_r^{"}$=.11) for the studies discussed above. The simulation result showing the effect of loss in the superstrate on AMC reflection phase, reflection coefficient magnitude and real part of impedance is shown in Figure 4 (a), (b) and (c), respectively. For the lossless superstrate (tanδ = 0), the real part of impedance is very high (3000 ohm) at the resonance frequency. The reflection coefficient magnitude is one and its phase is 0^0 at this frequency, i.e. the structure is showing AMC performance. As the value of tanδ increased to 0.4, the structure shows a drastic reduction in real part of impedance to 377 ohm which is same as the free space impedance. i.e. the structure is acting as a narrow band absorber[11] with reflection coefficient magnitude of -57 dB. Further increase in loss results in further reduction in real part of impedance and results in a perfect conductor like performance. The variation in impedance and reflection characteristics of AMC with superstrate loss is clear in the Smith chart plot shown in Figure 4(d).

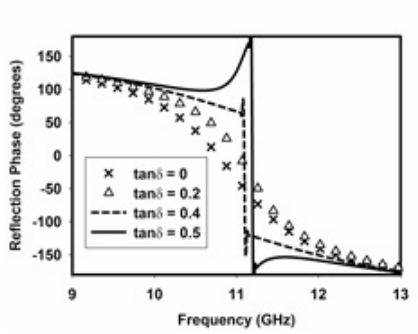

(a)

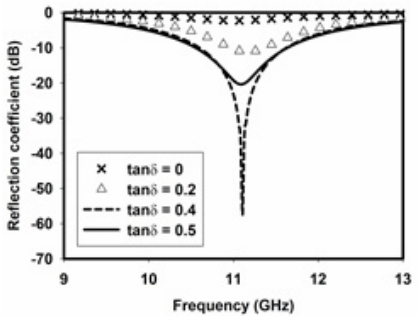

(b)

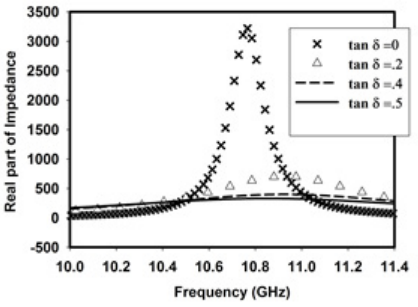

(c)

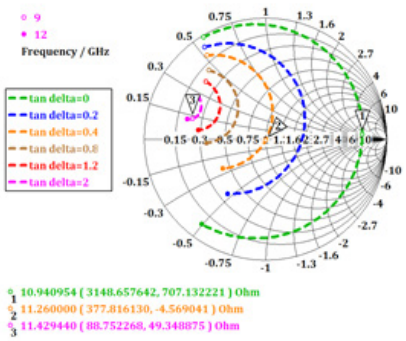

(d)

Figure 4. Simulation result showing the effect of superstrate loss on (a) reflection phase, (b) Reflection coefficient magnitude, (c) real part of impedance and (d) Smith chart (d = 8 mm, l = 5 mm, h_1 = 0.8 mm, h_2 = 0.8 mm, ε_r (sub) = 4.4-j*0.11, ε_{real} (super) = 4.4).

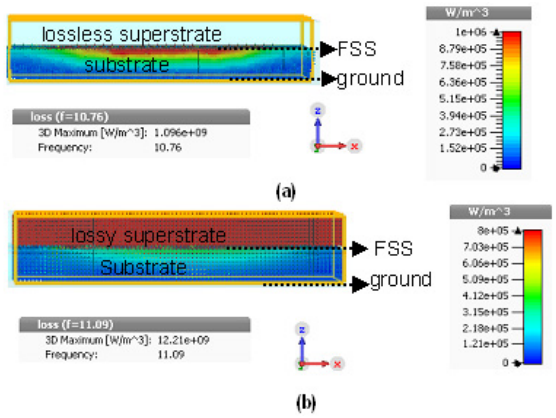

Figure 5. Distribution of power loss at resonance frequency (a) lossless superstrate at 10.76 GHz and (b) for lossy superstrate (tan δ =0.4) at 11.09 GHz.

Distribution of power loss for lossless and lossy superstrate at their resonance frequency is given in Figure 5 (a) and (b), respectively. For the case of lossy superstrate the power loss in the superstrate is very high which can be accounted for the absorber characteristics.

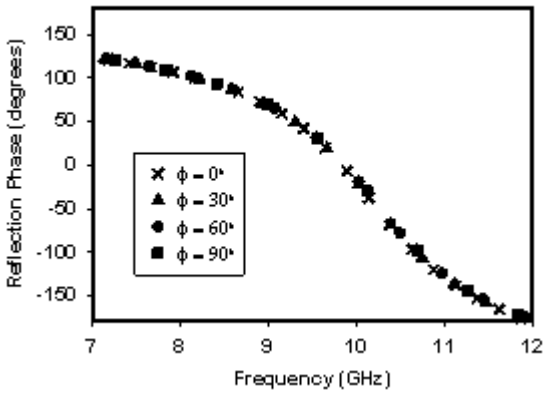

Figure 6. Simulation result showing the effect of polarization angle (ϕ) on AMC characteristic (d = 8 mm, l = 5 mm, h_1 = 0.8 mm, h_2 = 1.6 mm, ε_r (super) = 4.4-j*0.11, ε_r(sub) = 4.4-j*0.11, θ = 0^0).

3.3 Angle of Incidence and Polarization

To test the polarization independence and angular stability, the simulations are carried out for different polarization angle (ϕ) and incident angle (θ). When the polarization angle of incident wave is changing, the AMC response of the structure is nearly unchanged and the structure shows good polarization stability as shown in Figure 6. For different angles of incidence, the structure shows same AMC response for TM polarized and TE polarized waves as shown in Figure 7 (a) and (b), respectively. To further verify the angular stability, study is conducted for different angles of incidence at arbitrary polarization (ϕ = 30^0) and is shown in Figure7(c). This indicates that the structure has good angular stability for TE, TM and arbitrary polarization angles.

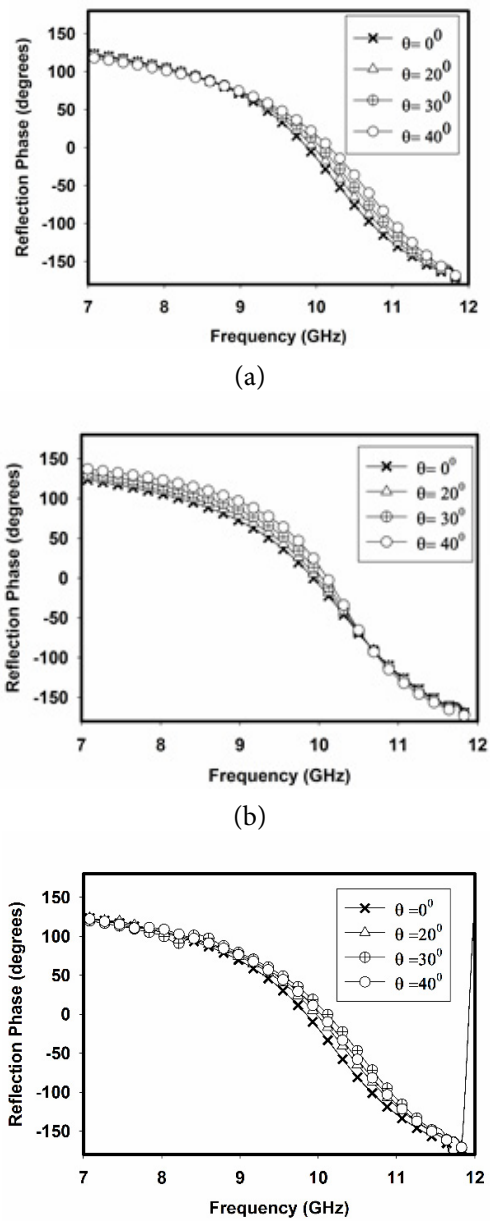

Figure 7. Effect of angle of incidence for (a) TM polarization, (b) TE-polarization and (c) ϕ = 30^0 (d = 8 mm, l = 5 mm, h_1 = 0.8 mm, h_2 = 1.6 mm, ε_r (super) = 4.4-j*0.11, ε_r (sub) = 4.4-j*0.11).

4. Measured Results

To validate the performance of the proposed structure, a 30 cm * 30 cm AMC structure is fabricated. Commercially available FR4 with thickness 0.8 mm, 1.6 mm and 2.4 mm are used as superstrate. The measurements are taken in an anechoic environment using R&S VNA ZVB20 and wide band transmit and receive horn antennas as shown in Figure 8. The reflectivity from a metal plate with same dimension as of the structure is taken for normalization.

The phase of the transmission coefficient of the structure with different superstrate thickness is measured and the measured reflection phases compared with simulated results are shown in Figure 9. The slight variation in measured and simulated results can be accounted for fabrication error or permittivity variation of commercially available FR4 substrate.

The polarization independence of the structure is also verified by TE and TM mode excitation of the AMC structure for normal incidence and is shown in Figure 10.

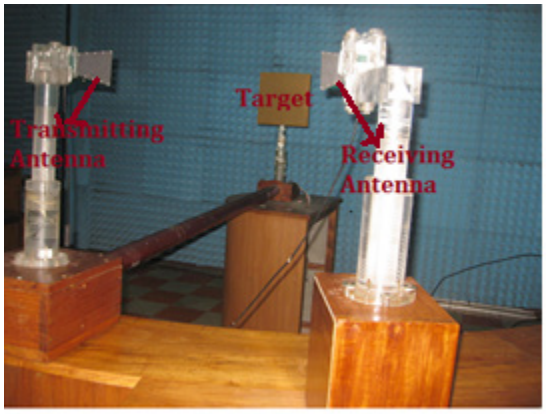

Figure 8. Photograph of the measurement setup.

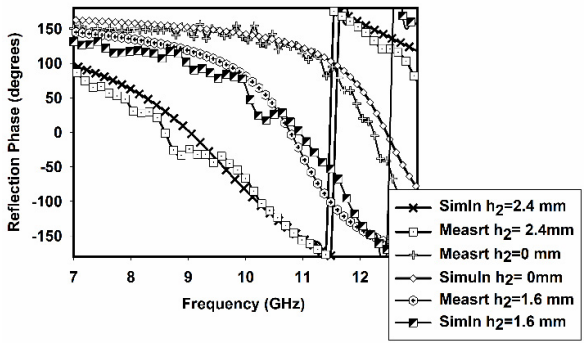

Figure 9. Comparison of measured and simulated results (d = 8 mm, l = 5 mm, h_1 = 0.8 mm, ε_r (super) = 4.4-j*0.11, ε_r(sub) = 4.4-j*0.11).

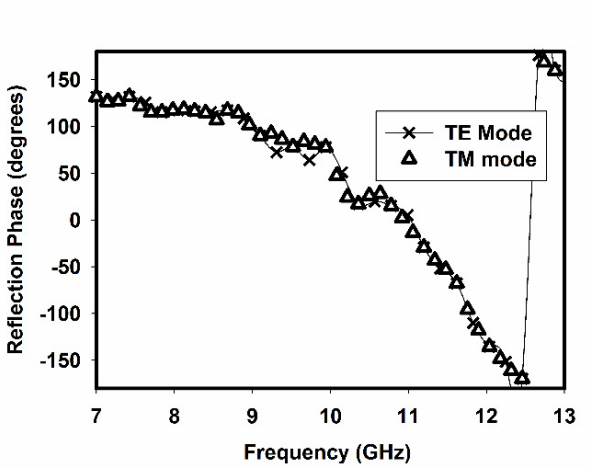

Figure 10. Reflection phase of the structure for TE and TM mode excitation for normal incidence (h_2 = 1.6 mm, ε_r (super) = 4.4-j*0.11, ε_r (sub) = 4.4-j*0.11).

5. Conclusion

In this paper, studies on the different characteristics of Artificial Magnetic Conductor (AMC) by superstrate loading are done. The AMC resonance frequency can be changed by loading superstrates of different thickness. This method is suitable for changing resonance frequency even after the fabrication of AMC. By using lossy superstrate, the AMC structure can be used as a narrowband absorber. A prototype is fabricated and the measured characteristics are found to be in good agreement with simulated results.

6. Acknowledgments

Authors would like to acknowledge the financial and infrastructural support from University Grants Commission and Department of Science and Technology, Government of India.

7. References

1. Sievenpiper D, Zhang L, Broas RFJ, Alexopolous NG, Yablonovitch E. High impedance electromagnetic surfaces in a forbidden frequency band. IEEE Transactions on Microwave Theory and Techniques. 1999; 47(11):2059–74. Crossref
2. Costa F, Monorchio A, Manara G. Analysis and design of ultrathin electromagnetic absorbers comprising resistively loaded high impedance surfaces. IEEE Transactions on Antennas and Propagation. 2010; 58(5):1551–8. Crossref

3. Kelly JR, Kokkinos T, Feresidis AP. Analysis and design of sub-wavelength resonant cavity type 2-D leaky-wave antennas. IEEE Transactions on Antennas and Propagation. 2008; 56(9):2817–25. Crossref
4. Sievenpiper D, Schaffner J. Beam steering microwave reflector based on electrically tunable impedance surface. Electronic Letters. 2002; 38(21):1237–8. Crossref
5. Costa F, Monorchio A, Talarico S, Valeri FM. An active high impedance surface for low profile tunable and steerable antennas. IEEE Antennas and Wireless Propagation Letters. 2008; 7:676–80. Crossref
6. Costa F, Monorchio A, Vastante GP. Tunable high-impedance surface with a reduced number of varactors. IEEE Antennas and Wireless Propagation Letters. 2011; 10:11–3. Crossref
7. Kern DJ, Werner DH, Monorchio A, Lanuzza L, Wilhelm MJ . The design synthesis of multiband magnetic conductors using high impedance frequency selective surfaces. IEEE Transactions on Antennas and Propagation. 2005; 53(1):8–17. Crossref
8. Wang XC, Zhao WS, Hu J, Yin WY. Reconfigurable terahertz leaky-wave antenna using graphene-based high-impedance surface. IEEE Transactions on Nanotechnology. 2015; 14(1):62–9. Crossref
9. Mckinzie WE III, Hurtado R, Klimczak W. Artificial magnetic conductor technology reduces size and weight for precision GPS antennas. Institute on Navigation National Technical Meeting; San Diego CA. 2002. p. 448–459.
10. Computer Simulation Technology. 2016.
11. Mol VAHL, Sasikumar SP, George DM, Lindo AO, Pushkaran NK, Aanandan CK. Radar cross section reduction property of high impedance surface on a lossy dielectric. Progress in Electromagnetic Research M. 2016; 46:19–28. Crossref